Application of Monte Carlo Techniques to the Potts Mode

Sam Van Den Ende, Odysseas Pattas

Abstract

This project investigates the phase transitions of the two-dimensional q-state Potts model. Using a modified Wolff cluster Monte Carlo algorithm, simulations were performed for $q = 2, 3, 4, 5, 6$ and lattice sizes $L = 10, 20, 30, 40, 50, 60, 70, 80$. The nature of the phase transitions, whether first-order or second-order, was determined by analyzing the behavior of magnetization and magnetic susceptibility as functions of temperature. The critical temperatures for each value of q were determined by fitting a Gaussian curve around the peak of the magnetic susceptibility for a lattice size $L = 80$. Notably, a significant difference in observables was identified between $q < 4$, exhibiting second-order transitions, and $q \geq 4$, exhibiting first-order transitions. An attempt was made to extract the critical exponents from collapse plots, but it was unsuccessful.

Introduction

The q-state Potts model

The q-state Potts model describes spin interaction within a lattice. Each spin state is represented as an equally spaced angle in a unit circle θ_n :

$$\theta_n = \frac{2\pi n}{q}, n = (0, 1, ...q - 1) \tag{1}$$

Each spin configuration is addressed by q and the Hamiltonian of the interaction is [1] :

$$H = -J \sum_{\langle i,j \rangle} \delta(s_i, s_j), (s_i, s_j) \in \{0, 1, ..., q - 1\} \tag{2}$$

Where J is the interaction strength constant, S_i is the spin state at site i, $\langle i, j \rangle$ denotes the sum over all nearest-neighbor pairs in the lattice and δ is the Kronecker delta. In our project we work on a two-dimensional system where the model is ferromagnetic $(J > 0)$, meaning that the spins tend to aligned in this nearest-neighbor interaction and the sum of spin site runs on a square lattice $L \times L$ with periodic boundary conditions are applied to minimize edge effects. During our calculation we will set $J/K_B = 1$. At the thermodynamic limit $(L- > \infty)$, the critical temperature T_c is [1] :

$$T_c = \frac{J/K_B}{\ln(1 + \sqrt{q})} \tag{3}$$

Observables Of The Model

Critical Temperature

Critical temperature T_c describes the temperature at which the state transforms from ordered to distorted phase. This phase transition depends on the value of q.

Magnetization

Magnetization describes how much allinged are the spins in the lattice configuration. Since the Potts model uses angles to describe the spin we are forced to represent those angles in the complex plane using the Euler formula: $S_i = e^{i\theta_i}$. Then the formula of the magnetization is :

$$M = |\frac{1}{N} \sum_{i=1}^{N} S_i| \tag{4}$$

Where: N runs for all spin configurations in the lattice.

Magnetic Susceptibility

The magnetic susceptibility, χ, is calculated based on the fluctuations in magnetization, defined as:

$$\chi = \frac{\langle M^2 \rangle - \langle M \rangle^2}{T} \tag{5}$$

Monte Carlo Cluster Algorithm for the q-Potts model

The cluster algorithm we use is an adaptation of the well-known Wolff cluster algorithm, modified to address the specifics of our problem. Since the observables we measure depend on the temperature, we aim to sample configurations according to the Boltzmann distribution. To achieve that, we introduce P_{bond} which represents the probability of creating a bond between two neighboring spins. In more detail, it determines whether two spins with the same state should be considered to be part of the same cluster:

$$P_{bond} = 1 - e^{-\beta J} \tag{6}$$

Where: $\beta = \frac{1}{K_B T}$ The algorithm starts by choosing a random seed state position in (i,j). If P_{bond} is greater than a uniform random number between 0 and 1, a bond is created, and the neighbor is added to the cluster. Repeat the bond formation step for all newly added spins until no more can be added to the cluster. Once the cluster is complete, flip all spins to a new random state. Choose the next seed spin uniformly randomly from all spins in the lattice, and repeat the process. This approach efficiently samples spin configurations while maintaining a detailed balance (Detailed Balance Proof), ensuring convergence to the equilibrium distribution. The temperature dependence of the bond probability P_{bond} influences the dynamics of cluster formation, ultimately driving the system toward different equilibrium phases.

Phase Transitions

The two-dimension ferromagnetic Potts model has a phase transition for all real values of $q \geq 1$ [2]. For $1 \leq q \leq 4$ there is a second-order transition, meaning that the magnetization will decrease continuously near the T_c while for $q \geq 4$ the transition becomes first-order, characterized by a discontinuous drop in magnetization at T_c, indicating a sharp phase change. Magnetic susceptibility χ plays a crucial role in distinguishing these types of transitions: For a second-order transition, χ diverges as $T \to T_c$, following a power law:

$$\chi \propto |T - T_c|^{-\gamma} \tag{7}$$

where γ is the critical exponent of susceptibility. Meanwhile, in first-order transitions, χ does not diverge but instead exhibits a finite peak near T_c.

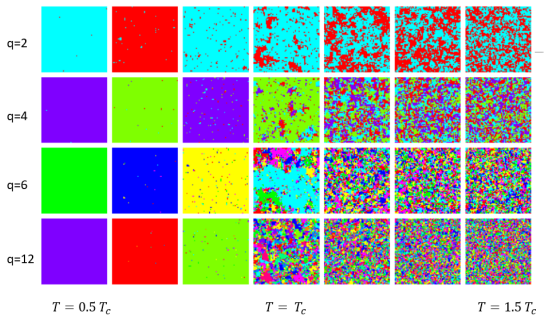

Figure 1: Simulation of the two-dimension Pott model using Monte Carlo methods on a 70×70 square lattice. Each color represents different spin configurations.

These differences in behavior of χ provide a clear signature of the type of phase transition occurs in the system. We will use this theoretical knowledge to investigate whether the Potts model exhibits the same behavior through numerical simulations and analysis of magnetization and susceptibility.

From figure 1 the change in phases is clear. For $q = 2, 4, 6, 12$, lattice size $L = 70$, and temperature $T = 0.5T_C$ the system is in an ordered state. As the temperature increases, clusters of different spins begin to form, and at even higher temperatures s $T = 1.5T_c$ the number of clusters increases significantly, driving the system into a disordered phase.

Methods

Equilibrium and Autocorrelation time

To determine the equilibration time of the system, we implemented a method that compares the magnetization of an initially ordered lattice with a disordered lattice. At the start of the process, the ordered lattice exhibits higher magnetization due to spin alignment. As Monte Carlo sweeps progress, the magnetization of both lattices evolves and eventually converges. The point at which the magnetizations become equal is defined as the equilibration time. This process is repeated for three independent runs to account for statistical variability, and the average number of sweeps required for equilibration is recorded as the final equilibration time.

To ensure that the samples used in our Monte Carlo simulation are statistically independent, we calculated the autocorrelation time of the system. First, the lattice is equilibrated by performing a

specified number of Wolff sweeps as mentioned before. Once equilibrium is reached, a sequence of lattice configurations is collected over 3000 steps, using magnetization as the observable. This procedure is repeated for a range of temperatures, and the autocorrelation time is reported in units of Monte Carlo sweeps, accounting for the average cluster size.

Simulation Of The Model

The simulation was performed for $q = 2, 3, 4, 5, 6$ and lattice sizes $L = 20, 30, 40, 50, 60, 70, 80$. For each value of q and L, the critical temperature is calculated using (3) to ensure that the temperature range studied focused on the critical phenomena of interest. The equilibrium time, in terms of the number of Monte Carlo sweeps, was then calculated at the critical temperature.

For the autocorrelation time, the temperature range used is $[0.7 \times T_C, 1.3 \times T_C]$. To calculate the magnetization and magnetic susceptibility, 100 samples were taken for each temperature, using thinning to avoid correlated observables. The thinning time was set as $max(1, [\tau])$, where τ is the autocorrelation time,ensuring that at least one sweep separates consecutive samples, even for small values of τ.

For error estimation, jackknife batching was employed with a batch size of 20. Using this approach, we ensure that the sampled observables are uncorrelated and that the error estimation for these observables is robust.

Results

Monte Carlo Results

Here we illustrate the magnetization and magnetic susceptibility of each q for $L = 30, 50, 80$ supplementary plots for different values of q and L can be found in Appendix (Supplementary plots).

In Figure 2 it is evident that as the lattice size L increases, the first-order transition phenomenon becomes more evident. Especially for L = 80 and for the values of q = 5 and q = 6 there is a noticeable jump in magnetization near the critical temperature, indicating a sharp phase transition. In contrast, for lower values of $q = 2$ and $q = 3$ the transition is smoother and more continuous, consistent with second-order phase transitions.

The magnetic susceptibility plots 3 illustrate that as the lattice size increases, the peaks in magnetic susceptibility become sharper and more pro-

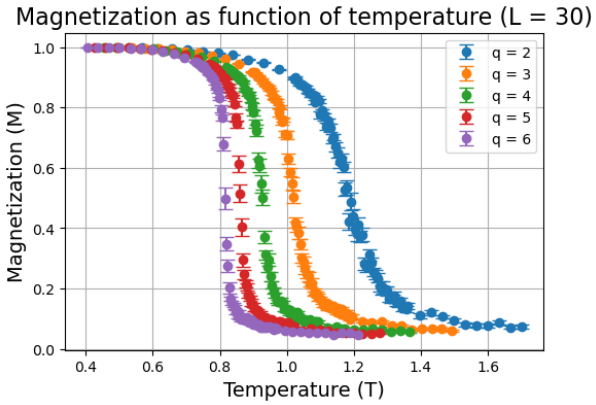

(a) L = 30

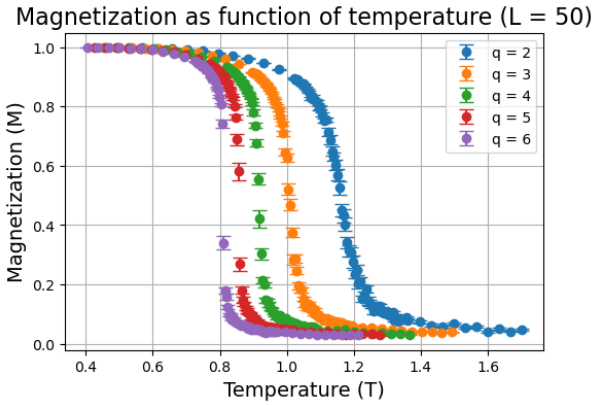

(b) L = 50

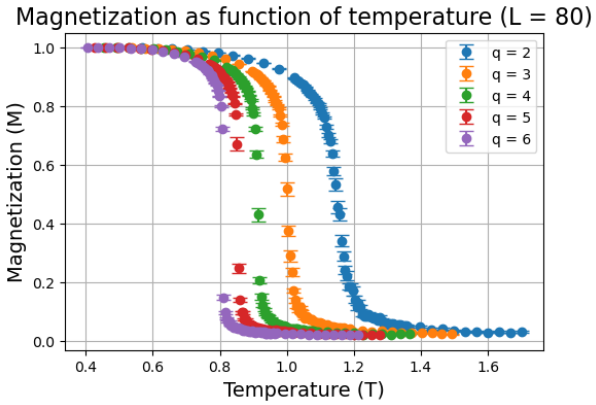

(c) L = 80

Figure 2: Magnetization as a function of temperature for $L = 30, 50, 80$ and $q = 2, 3, 4, 5, 6$.

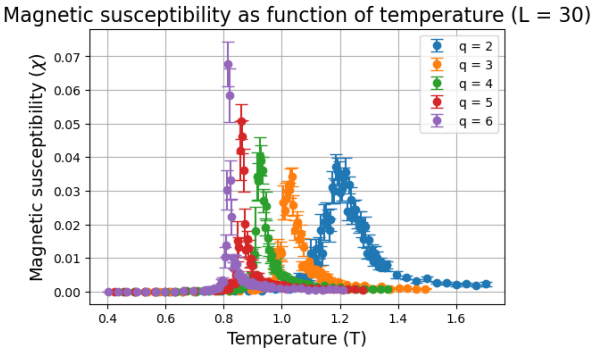

(a) L = 30

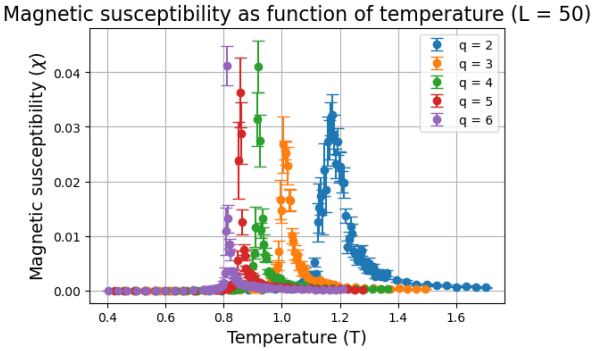

(b) L = 50

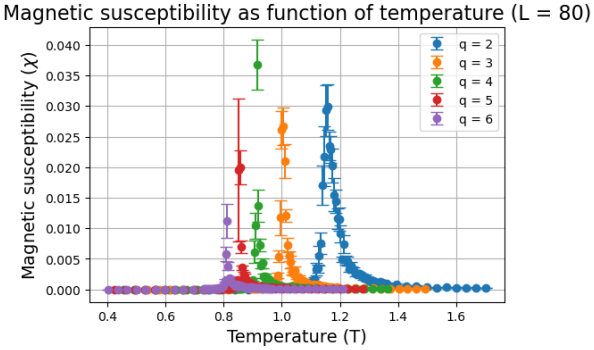

(c) L = 80

Figure 3: Magnetic susceptibility as a function of temperature for $L = 30, 50, 80$ and $q = 2, 3, 4, 5, 6$.

nounced, especially for higher values of q. This behavior indicates a first-order phase transition, as the susceptibility exhibits a sharp divergence near the critical temperature. For lower values of $q = 2$ and $q = 3$ the peaks are broader and smoother as we would expect in a second-order phase transition. Also, from these plots finite-scaling is shown with sharper transitions emerging as lattice size increases.

Estimation of Critical Temperature

To estimate the critical temperature for each q value, we focused solely on $L = 80$, as its large size better reflects the behavior of the system with reduced finite-size effects. The critical temperature was determined by fitting a Gaussian curve around the peak of the magnetic susceptibility plotted as a function of temperature. This method is particularly effective for second-order transitions, where the peak is broader and smoother, resembling a bell curve.

The uncertainty in the critical temperature was estimated from the covariance matrix obtained during the Gaussian fitting. Specifically, the standard error of the fitted mean temperature was calculated as the square root of the corresponding diagonal element in the covariance matrix.

We then compared our results with the theoretical values obtained at the thermodynamic limit ($L- > \infty$) using 3.

q-value	T_c(Fitted)	T_c (Theoretical)
2	1.161 ± 0.00143	1.1346
3	1.005 ± 0.00064	0.9950
4	0.915 ± 0.00039	0.9102
5	0.854 ± 0.00031	0.8515
6	0.811 ± 0.00032	0.8076

Table 1: Critical temperatures obtained from the curve fitting compare to the theoretical values.

From 1 and 4, it is evident that the values of T_C we obtained closely resemble the theoretical ones. Of course, these values cannot be identical, as the theoretical equation used refers to the infinite-size lattice limit, while we used a 80×80 square lattice.

Lattice Size Effects on Observables

The size of the lattice plays a crucial role in determining the accuracy of observables in finite-size scaling studies. Smaller lattice sizes are more susceptible to finite-size effects, leading to significant

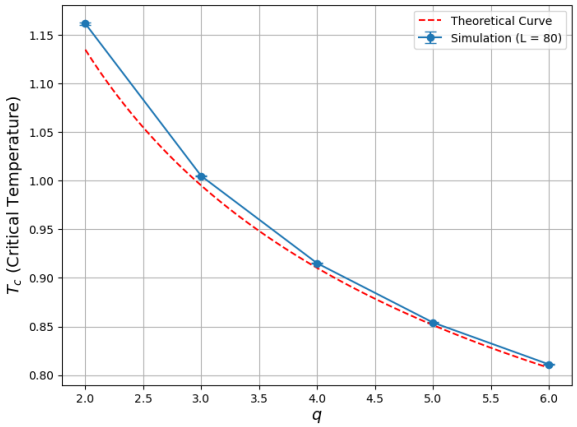

Figure 4: Estimated critical temperatures compared to its theoretical values for each q.

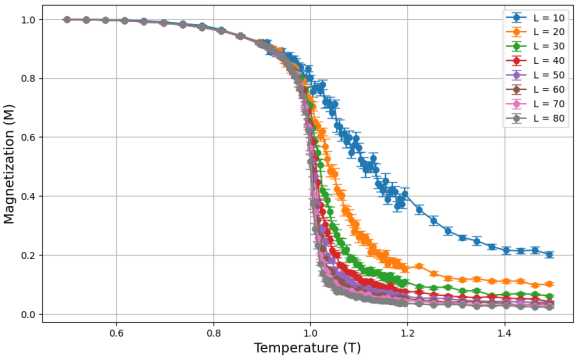

Figure 5: Collapse plot for $q = 3$ and $L = 10, 20, 30, 40, 50, 60, 70, 80$. Note the difference between $L = 10$ and the rest of the curves.

deviations from the expected behavior in the thermodynamic limit. This is evident from 5, where the behavior of $L = 10$ diverges noticeably from the rest of the data. These deviations result in increased noise and unreliable trends that do not accurately reflect the system's critical behavior. To minimize the influence of finite-size effects and improve the reliability of our results, the case of $L = 10$ was excluded from the estimation of the critical components.

Critical Exponents

Inspired by the lectures, we first determined the Hassford dimension, d_H, for each value of q. However, in this paper, we focus on presenting the results for the case of $q = 3$. The temperature and susceptibility were rescaled using the finite-size scaling relations:

$$r = (T - T_c)L^{1/d_H}, \quad \chi_{\text{scaled}} = \chi L^{-(1-1/d_H)}.$$

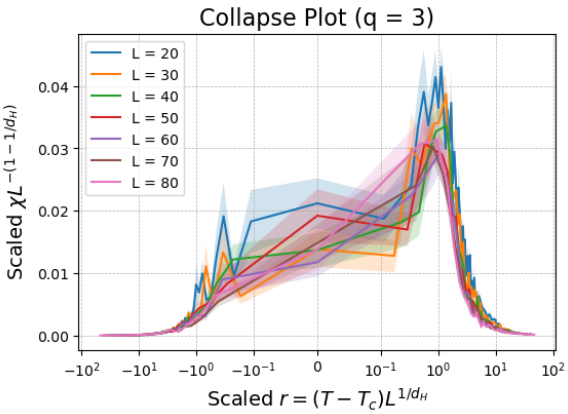

Figure 6: Collapse plot of scaled magnetic susceptibility versus scaled temperature for $q = 3$.

Simulations were performed for $q = 2, 3, 4, 5, 6$ and lattice sizes $L = 20, 30, 40, 50, 60, 70, 80$. For each value of q, d_H was determined by minimizing the collapse error of the rescaled susceptibility curves.

To extract the critical exponents ν and γ for the two-dimensional q-state Potts model, we utilized the finite-size scaling relationship of the magnetic susceptibility, χ, at the critical temperature T_c. Specifically, a log-log regression was performed to compute the ratio γ/ν from the susceptibility scaling relation:

$$\chi \sim L^{\gamma/\nu}.$$

For each lattice size, the susceptibility at T_c was extracted, and a linear regression was applied to $\log(\chi)$ vs. $\log(L)$. The slope of the resulting fit corresponds to γ/ν.

Once γ/ν was determined, the critical exponents ν and γ were calculated using the previously obtained Hassford dimension d_H through the relationships:

$$\nu = \frac{1 + \gamma/\nu}{d_H}, \quad \gamma = \nu \cdot \frac{\gamma}{\nu}.$$

The collapse plot of the scaled magnetic susceptibility versus scaled temperature 6 exhibits significant overlap of the curves for all lattice sizes L, indicating that the scaling relation accurately reflects the system's behavior. However, the overlap is significantly broad, and the high error estimates from small lattice sizes ($L = 10, 20$) due to finite-size effects make the estimation of the Hassford dimension d_H challenging.

From 7, it is evident that the slope obtained is not accurate. Using this method, we calculated

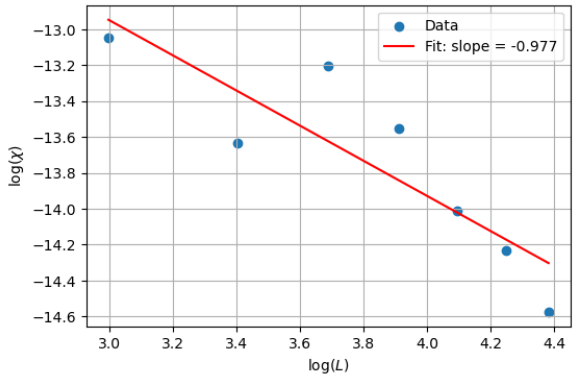

Figure 7: Log-log plot of size dependence of the susceptibility at the critical temperature.

$d_H = 0.65$ and the critical exponents $\gamma = 2.923$ and $\nu = -1.298$. These values significantly deviate from those reported in the literature [3], where for $q = 3$, $\gamma = 1.435$ and $\nu = 0.827$. Furthermore, the slope in the log-log plot is expected to be positive, suggesting an error in the implementation of the method.

Conclusion

In this work, we performed simulations of the q-state Potts model using the Monte Carlo algorithm for $q = 2, 3, 4, 5, 6$ and lattice sizes $L = 10, 20, 30, 40, 50, 60, 70, 80$. These simulations revealed critical phenomena that are qualitatively different for $q < 4$ and $q \geq 4$, corresponding to second-order and first-order phase transitions, respectively. Additionally, we estimated the critical temperature for each value of q.

Finite-size effects were evident in the collapse plots, particularly for smaller lattice sizes, which posed challenges in computing the Hassford dimension and critical exponents for the case of $q = 3$. While some progress was made, further refinement or debugging is required to achieve reliable results.

References

[1] Fa-Yueh Wu. "The potts model". In: *Reviews of modern physics* 54.1 (1982), p. 235.

[2] Vincent Beffara and Hugo Duminil-Copin. "The self-dual point of the two-dimensional random-cluster model is critical for q 1". In: *Probability Theory and Related Fields* 153.3 (2012), pp. 511–542.

[3] AA Caparica, Salviano A Leão, and Claudio J DaSilva. "Static critical behavior of the q-states Potts model: High-resolution entropic study". In: *Physica A: Statistical Mechanics and its Applications* 438 (2015), pp. 447–453.

Appendix

Detailed Balance Proof

To demonstrate that the cluster algorithm satisfies detailed balance, we must show that the transition probabilities between any two configurations C and C' satisfy:

$$P(C)W(C \to C') = P(C')W(C' \to C),$$

where: $P(C)$ and $P(C')$ are the Boltzmann probabilities of configurations C and C' and $W(C \to C')$ is the transition probability from C to C'.

The Potts model assigns the Boltzmann probability to a configuration C as:

$$P(C) = \frac{1}{Z} e^{-\beta H(C)},$$

where Z is the partition function, $\beta = 1/(k_B T)$, and $H(C)$ is the Hamiltonian of configuration C.

The transition probability $W(C \to C')$ can be divided into two steps: Forming a cluster based on the bond probability $P_{\text{bond}} = 1 - e^{-\beta J}$ and flipping all spins in the cluster to a new spin state chosen uniformly at random.

Let $\mathcal{C}$ be the cluster formed in C. The probability of forming this cluster depends only on P_{bond}, ensuring that the cluster respects the Boltzmann weight of C.

Since the probability of forming a cluster and flipping it is symmetric, the transition probabilities satisfy:

$$W(C \to C') = W(C' \to C).$$

Given that $P(C) \propto e^{-\beta H(C)}$ and the Hamiltonian is invariant under cluster flipping, we have:

$$P(C)W(C \to C') = P(C')W(C' \to C).$$

Supplementary plots

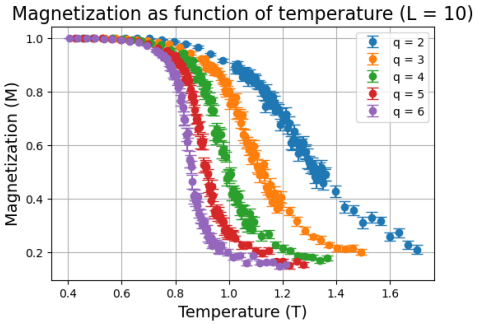

(a) L = 10

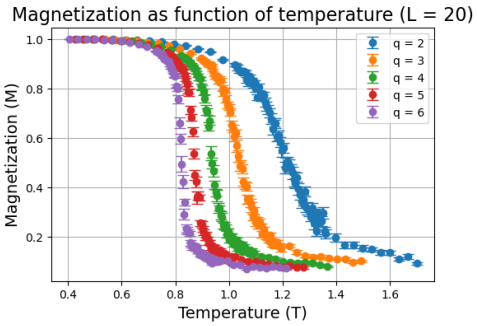

(b) L = 20

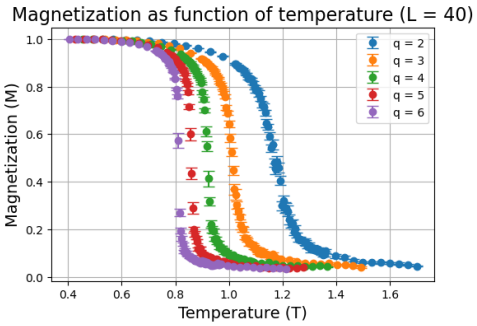

(c) L = 40

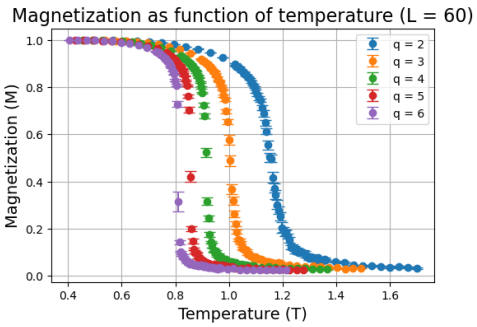

(d) L = 60

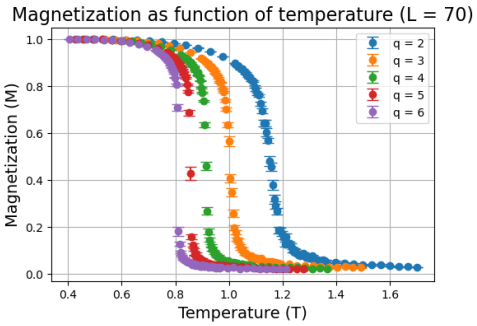

(e) L = 70

Figure 8: Magnetization as a function of temperature for $L = 10, 20, 40, 60, 70$ and $q = 2, 4, 5, 6$.

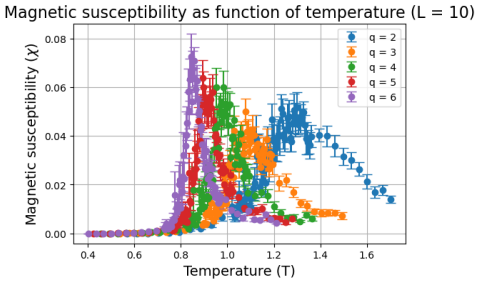

(a) L = 10

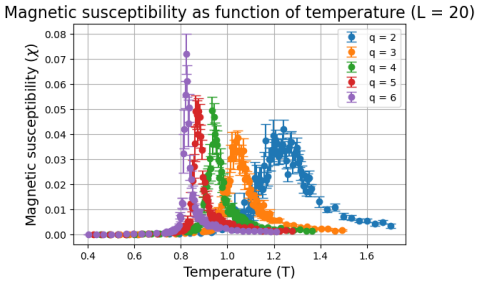

(b) L = 20

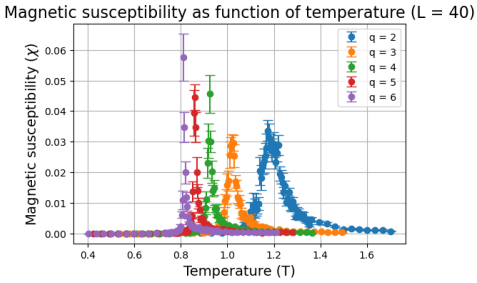

(c) L = 40

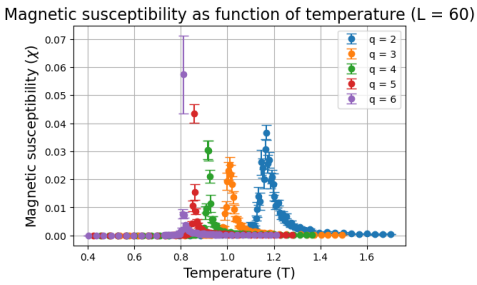

(d) L = 60

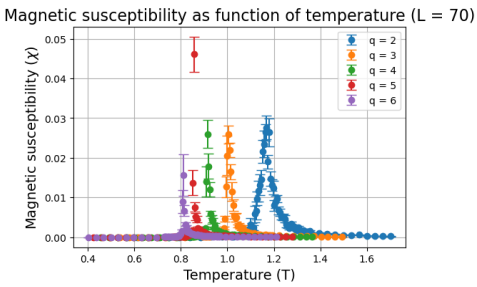

(e) L = 70

Figure 9: Magnetic susceptibility as a function of temperature for $L = 10, 20, 40, 60, 70$ and $q = 2, 4, 5, 6$.

Individual contributions

Regarding individual contributions, particularly in the coding aspect, both attempted the same tasks independently and compared their results to determine which method was more accurate. In almost all cases, the Sam's Van Den Ende proved to be more effective.

Summary of Contributions:

- **Research for the project:** Both
- **Coding:** Both (Majority by Sam Van Den Ende)
- **Data analysis:** Both
- **Presentation:** Odysseas Pattas
- **Report:** Odysseas Pattas
- **Data collection:** Both